doi: 10.12029/gc20190429004

王晓地,孙传敏,贾小辉,张利国,周岱. 2023. 桂东南马山玄武岩的年代学、地球化学及岩石成因:对华南地区印支期构造背景的制约[J]. 中国地质, 50(2): 573−585.

Wang Xiaodi, Sun Chuanmin, Jia Xiaohui, Zhang Liguo, Zhou Dai. 2023. Geochronology, geochemistry, and petrogenesis of the Mashan basalt in southeast Guangxi Province: Constraints on the Indosinian tectonic setting of South China[J]. Geology in China, 50(2): 573−585(in Chinese with English abstract).

桂东南马山玄武岩的年代学、地球化学及岩石成因:对华南地区印支期构造背景的制约

王晓地[1,2],孙传敏[3],贾小辉[1,2],张利国[1,2],周岱[1,2]

(1. 中国地质调查局武汉地质调查中心,湖北 武汉 430205;2. 中国地质调查局花岗岩成岩成矿研究中心,湖北 武汉 430205;3. 成都理工大学地球科学学院,四川 成都 610059)

提要:【研究目的】桂东南马山杂岩体北部出露的印支期玄武岩,是研究华南印支运动的关键岩石探针。目前关于马山玄武岩的研究资料较少,制约了对华南地区大地构造背景演化的认识。**【研究方法】**本文对马山玄武岩开展了锆石U−Pb年代学、岩石地球化学、Sr−Nd同位素研究。**【研究结果】**玄武岩的LA−ICPMS锆石U−Pb年龄为 (246.7±1.5) Ma,MSWD=0.16。岩石富碱((K_2O+Na_2O)=5.21%~8.02%)、富钾(K_2O=2.59%~4.96%),为钾质粗面玄武岩,稀土元素特征为轻稀土富集型,微量元素特征为富集大离子亲石元素(Rb、Ba、K、Pb、LREE),亏损高场强元素(Nb、Ta、P、Ti、HREE),Sr−Nd同位素显示具有EMⅡ富集地幔端元的特征。**【结论】**马山玄武岩符合钾玄岩系列的岩石特点,其岩浆作用以分离结晶为主,无明显的地壳混染,其源区为受俯冲壳源物质释放的流体交代作用形成的含金云母石榴子石的富集地幔(>80 km)源区。马山玄武岩产于板内环境,其形成可能与印支期逆冲−推覆构造后期的伸展作用有关,由于伸展作用产生有利空间,造成玄武质岩浆上涌喷发形成玄武岩。

关 键 词:年代学;地球化学;岩石成因;马山玄武岩;桂东南;地质调查工程;华南

创 新 点:马山玄武岩形成年龄为(246.7±1.5) Ma,产于板内环境,其形成可能与印支期逆冲−推覆构造后期的伸展作用有关。

中图分类号: P597$^+$.3; P581 **文献标志码:** A **文章编号:** 1000−3657(2023)02−0573−13

Geochronology, geochemistry, and petrogenesis of the Mashan basalt in southeast Guangxi Province: Constraints on the Indosinian tectonic setting of South China

WANG Xiaodi[1,2], SUN Chuanmin[3], JIA Xiaohui[1,2], ZHANG Liguo[1,2], ZHOU Dai[1,2]

(1. *Wuhan Center, China Geological Survey, Wuhan* 430205*, Hubei, China;* 2. *Research Center of Granitic Diagenesis and Mineralization, China Geological Survey, Wuhan* 430205*, Hubei, China;* 3. *College of Earth Sciences, Chengdu University of Technology, Chengdu* 610059*, Sichuan, China*)

收稿日期: 2019−04−29;**改回日期:** 2019−09−10

基金项目: 中国地质调查局项目(1212710610714、12120120512、DD20190811、DD20230226)资助。

作者简介: 王晓地,男,1974年生,高级工程师,从事岩石学和矿床学调查和研究工作;E−mail: 178372234@qq.com。

Abstract: This paper is the result of geological survey engineering.

[Objective] Indosinian basalt, exposed in the northern part of the Mashan Complex in southeast Guangxi province, is a key rock probe for the study of Indosinian movement in South China. It has been seldom researched so far, which restricts the recognition of evolution of tectonic setting in South China. **[Methods]** We carried out zircon U−Pb geochronology, geochemistry, Sr−Nd isotopic geochemistry and petrogenesis of the Mashan basalt. **[Results]** The results show that the LA−ICPMS zircon U−Pb age of the Mashan basalt is (246.7±1.5) Ma, (MSWD=0.16). The basalt belongs to potassium trachybasalt with high alkali (K_2O+Na_2O=5.21%−8.02%), especially potassium (K_2O=2.59%−4.96%), and is enriched in large ion lithophile elements (Rb, Th, U, K, Pb, LREE) but depleted in high field strength elements (Nb, Ta, P, Ti, HREE). The Sr−Nd isotopes of the Mashan basalt have affinity with enriched mantle (EMⅡ). **[Conclusions]** The geochemical characteristics of the Mashan basalt exhibit shoshonitic features, and is mainly a product through fractional crystallization without obvious crustal contamination. It was probably derived from partial melting of phlogopite− and garnet−bearing lithospheric mantle (>80 km), which was metasomatized by subducted crustal materials. The basalt is developed in an intraplate setting, likely to be shaped by magmatic eruption and intrusion upwards through favorable space created by the extension in the later stage of the Indosinian thrust−nappe structure.

Key words: geochronology; geochemistry; petrogenesis; Mashan basalt; southeastern Guangxi Province; geological survey engineering; South China

Highlights: The formation age of the Mashan basalt is (246.7±1.5) Ma. It is produced in an intraplate extensional setting, probably related to the extension in the later stage of the Indosinian thrust−nappe structure.

About the first author: WANG Xiaodi, male, born in 1974, senior engineer, engaged in the investigation and study of petrology and mineral deposits; E−mail: 178372234@qq.com.

Fund support: Supported by the projects of China Geological Survey (No.1212710610714, No.12120120512, No.DD20190811, No. DD20230226).

1 引 言

玄武岩原生岩浆来自于上地幔,成分与地幔源岩关系十分密切,其岩浆的产生往往又与裂谷扩张、板块俯冲消减、地幔的深部作用等过程有关(徐义刚,2006;Nielsen et al., 2006;Campbell, 2007;厉子龙等,2008)。碱性玄武岩因其产出的特殊构造背景而备受关注(王岳军等,2004;余心起等,2005;陈立辉等,2012;赵慧等,2015)。华南印支期岩浆岩以发育强过铝—过铝质花岗岩为特征,同期基性火山岩极少出露,代表的有湖南道县虎子岩玻基辉橄岩$^{40}Ar-^{39}Ar$坪年龄为204 Ma(赵振华等,1998)、宁远碱性玄武岩年龄为212.3 Ma(刘勇等,2010)及武夷山地区霓辉石正长岩年龄为242 Ma(Wang et al., 2003)。

马山杂岩为一个多次岩浆活动形成由超基性、基性、中酸性岩组成的中生带复杂岩体(王晓地,2013)。玄武岩分布于杂岩体的北部,由浅层相的玄武玢岩逐步过渡到喷出相的玄武岩,因其侵入泥盆系,同时又被早燕山期花岗斑岩侵入,故认为其时代为印支期。但目前还没有与之相协调的同位素精确年龄。前人对马山杂岩也做过系统研究,但存在一定的分歧,吴根耀和李曰俊(2011)认为马山杂岩中的印支期玄武岩属亚速尔型洋岛玄武岩,为沿灵山断裂曾发育过洋盆提供了直接的地质依据,成为恢复现已消失了的洋盆的一个重要判据;广西壮族自治区区域地质调查研究院(2006)❶认为马山复式岩体为板内型钾玄岩,其形成构造环境与岛弧无关;郭新生等(2001)认为马山基性岩源区为交代地幔的辉长岩浆在地壳深部分异而形成的,马山花岗岩由幔源岩浆加热地壳使之熔融的壳源岩浆形成并伴有与幔源岩浆的混合;Li et al.(2000)认为马山玄武岩是典型的板内岩浆岩,与岛弧环境不存在成因联系,表明桂东南钾玄质岩石很可能是亏损的软流圈地幔和富集的岩石圈地幔岩浆混合的产物。本文拟报道桂东南马山玄武岩锆石U−Pb精确年龄,结合地球化学及Sr−Nd同位素资料,探讨其岩石成因和形成的构造背景,为华南地区印支期的动力学背景研究提供依据。

2 岩体地质特征

马山杂岩位于桂东南六万大山,出露面积约为93 km^2(图1),大地构造上位于特提斯构造域和环太平洋构造域的交汇处,同时又处于扬子与华夏两大块体接合部位即"钦杭结合带"内。岩体侵位于

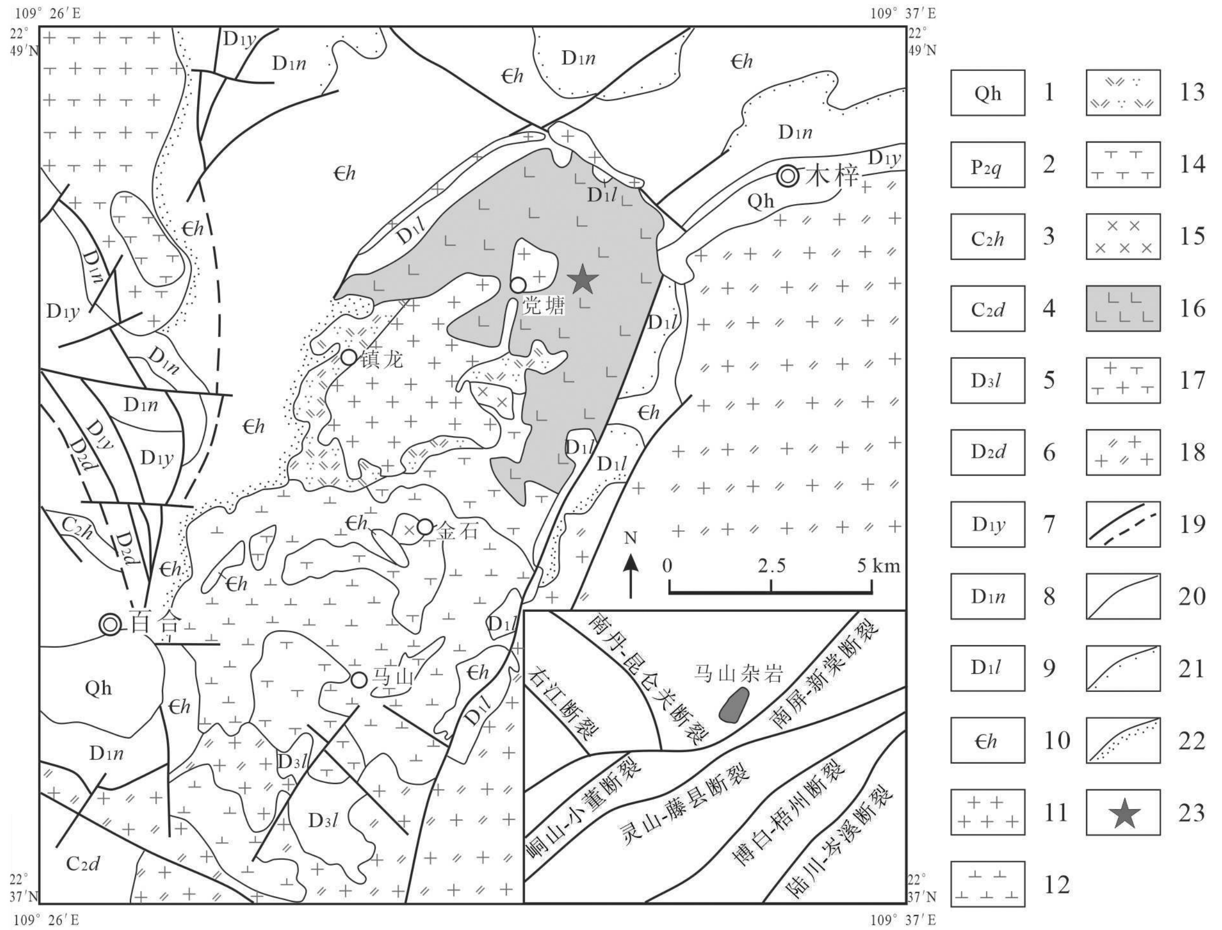

图1 马山杂岩体地质图(据广西壮族自治区区域地质调查研究院,2006[❶]修改)

1—全新统;2—茅口组;3—黄龙组;4—大埔组;5—榴江组;6—东岗岭组;7—郁江组;8—那高岭组;9—莲花山组;10—黄洞口组;11—花岗斑岩;12—正长岩;13—石英二长岩;14—闪长岩;15—辉石岩;16—玄武岩;17—花岗闪长岩;18—二长花岗岩;19—断层;20—地质界线;21—角度不整合界线;22—角岩、矽卡岩化;23—玄武岩年龄采样点

Fig.1 Geological map of the Mashan Complex (modified from the Guangxi Zhuang Autonomous Region Institute of Regional Geological Survey, 2006[❶])

1−Holocene; 2−Maokou Formation; 3−Huanglong Formation; 4−Dapu Formation; 5−Liujiang Formation; 6−Donggangling Formation; 7−Yujiang Formation; 8−Nagaoling Formation; 9−Lianhuashan Formation; 10−Huangdongkou Formation; 11−Granite porphyry; 12−Syenite; 13−Quartz monzonite; 14−Diorite; 15−Pyroxenite; 16−Basalt; 17−Granodiorite; 18−Monzogranite; 19−Fault; 20−Geological boundary; 21−Angular unconformity; 22−Hornfels, skarnization; 23−Sampling location

寒武系、泥盆系和印支期大容山岩体中,为一个多次岩浆活动形成由超基性、基性、中酸性岩组成的中生代复杂岩体(王晓地,2013)。玄武岩分布于岩体的北部,由浅层相的玄武玢岩逐步过渡到喷出相的玄武岩,出露面积约30 km^2。

玄武岩为深灰色,具斑状结构、基质具间粒间隐结构,以块状和气孔状构造为主。斑晶为斜长石(30%)、辉石(15%)、少量橄榄石及角闪石,基质为斜长石(35%)、辉石(15%)与金属矿物(4%),含少量副矿物。斜长石斑晶呈半自形板状、常见聚片双晶、卡钠复合双晶;辉石斑晶呈粒状、短柱状,被碳酸盐化只保留轮廓;橄榄石斑晶呈粒状,被伊丁石化只保留轮廓;角闪石斑晶呈柱状、粒状,绿泥石化只保留轮廓。基质中斜长石呈板条状、粒状,具有聚片双晶,辉石呈粒状分布在长石间隙中,由于碳酸盐化,只保留辉石轮廓。金属矿物主要以磁铁矿为主,副矿物为磷灰石、锆石(图2)。

3　锆石同位素测年

锆石测年选择玄武岩(Mszy−7)为测试对象,年

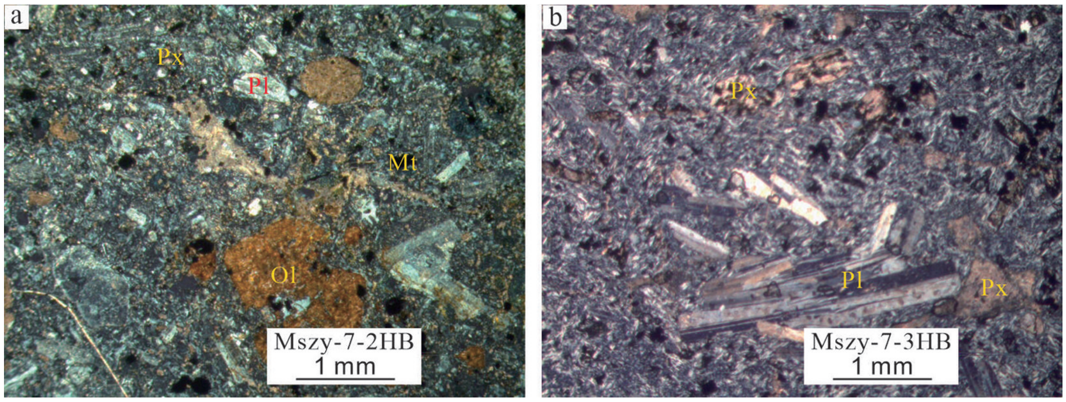

图2 马山玄武岩显微照片
Pl—斜长石；Px—辉石；Ol—橄榄石；Mt—磁铁矿
Fig.2 Micrographs of the Mashan basalt
Pl–Plagioclase; Px–Pyroxene; Ol–Olivine; Mt–Magnetite

代学样品采自南宁市横县步头村（地理坐标为22°45′33″N，109°35′22″E），锆石样品挑选由国土资源部河北省地质矿产局廊坊实验室完成，锆石阴极发光（CL）照相在中国地质大学JXA−8100电子探针仪上完成。LA−ICPMS锆石U−Pb年龄测定在西北大学大陆动力学国家重点实验室的Agilent7500型ICPMS上进行。仪器分析步骤及分析结果数据处理参照文献（Yuan et al., 2003）。

玄武岩锆石多数呈长柱状，晶形较完好，颗粒大小一般为50 μm×100 μm，韵律环带发育。在CL图像上大部分核部和边部差异不明显（图3）。所测锆石的18个分析点中Th含量为191×10^{-6}~838×10^{-6}，U含量为508×10^{-6}~3348×10^{-6}，Th/U比值为0.16~1.19，均表现出岩浆锆石的特点。其中12和15号点为老锆石，$^{207}Pb/^{206}Pb$年龄分别为1070 Ma和1650 Ma，与$^{206}Pb/^{238}U$年龄不一致，可能为部分Pb丢失所致；3号点年龄偏老，$^{206}Pb/^{238}U$年龄为464 Ma；2、16、17和19号点的$^{206}Pb/^{238}U$年龄变化于262~288 Ma，可能代表了早期的岩浆活动；5号点的$^{206}Pb/^{238}U$年龄偏低，为133 Ma，可能与区内早白垩世的变质作用有关。所测试的其余10个分析点$^{206}Pb/^{238}U$年龄相对集中，主体变化于245~248 Ma，落在U−Pb谐和线上或其附近（图3），获得$^{206}Pb/^{238}U$年龄的加权平均值为（246.7±1.5）Ma，MSWD=0.16，代表了玄武岩的形成年龄（表1）。同时玄武岩侵入泥盆纪地层，又被早燕山期时代为185.2 Ma的花岗斑岩侵入（王晓地，2013），故认为其形成时代为印支期。

4 岩石地球化学特征

玄武岩的主量元素分析在中国地质调查局武汉地质调查中心完成（表2），分析方法为：Si和烧失量采用重量法，Al和Fe^{2+}采用容量法，Fe^{3+}、Ti和P采用分光光度法，K、Na、Ca、Mg和Mn采用原子吸收光谱法；微量元素分析在核工业北京地质研究院分析测试研究中心完成，微量元素采用HR−ICP−MS (Element I)分析完成（表2）；Sr、Nd同位素分析用中国地质调查局武汉地质调查中心MAT261及Triton质谱仪分析完成（表3），实验流程以及标准样品测定按照Sm−Nd同位素实验方法完成（王银喜等，1988）。

4.1 主量元素

玄武岩呈基性（SiO_2=46.02%~51.56%），碱性程度较强（δ=5.21~8.02），岩石总体富碱（ALK=5.21%~8.02%）、富钾（K_2O=2.59%~4.96%）、K_2O大于Na_2O（个别样品除外）（K_2O/Na_2O=1.07~1.62），铝含量较高（Al_2O_3=12.01%~14.88%），$Mg^{\#}$值高（35.11~56.09），钛含量高（TiO_2=1.24%~2.15%），铁含量较高（($FeO+Fe_2O_3$)=10.80%~12.66%）。在火山岩TAS分类图解中主要落在粗面玄武岩区、少数落在玄武粗安岩及碱玄岩区（图4a），SiO_2-K_2O图解落在钾玄质系列岩石范围内（图4b），岩石属钾质粗面玄武岩。

4.2 稀土元素

玄武岩稀土元素总量（∑REE）为150.98×10^{-6}~254.89×10^{-6}，轻稀土元素富集，稀土元素球粒陨石标

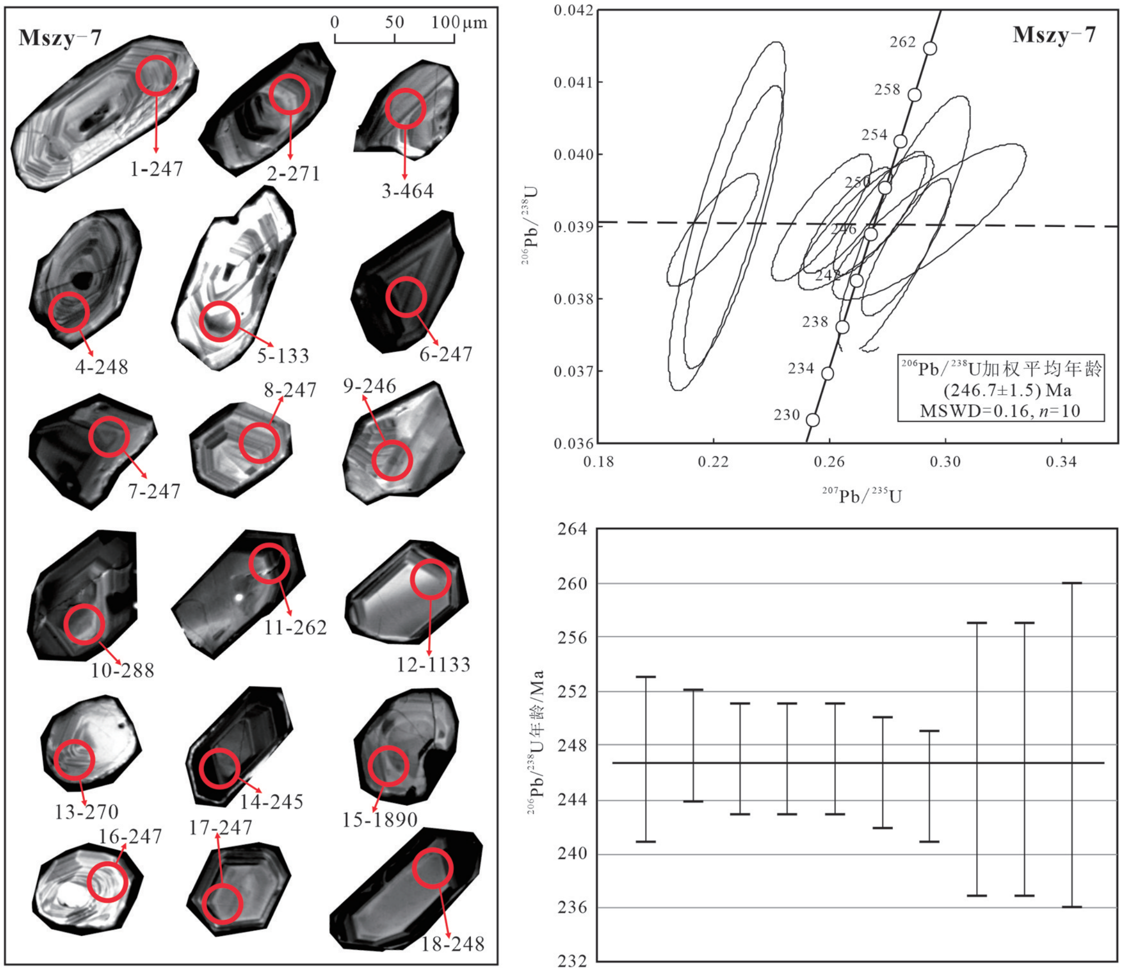

图3 马山玄武岩锆石阴极发光图像及锆石U-Pb谐和图
Fig.3 CL images and U-Pb concordia diagram of zircons from the Mashan basalt

准化配分图上表现为右倾趋势(图5a),轻、重稀土元素比值(LREE/HREE)为6.94~9.87,$(La/Yb)_N$值介于8.43~14.75;具轻微的Eu负异常,δEu值介于0.85~0.95。

4.3 微量元素

在微量元素原始地幔标准化蛛网图上(图5b),玄武岩均表现为富集大离子亲石元素(LILEs,Rb、Ba、K、Pb、LREE),亏损高场强元素(HFSE,Nb、Ta、P、Ti、HREE),而无明显的Zr亏损。

4.4 Sr-Nd同位素

玄武岩全岩Sr-Nd同位素计算使用Geokit软件完成(路远发和李文霞,2021)。Sr-Nd同位素组成相对变化较大(表3),Sr同位素组成较均一,I_{Sr}=0.704597~0.704834;Nd同位素变化较大,$\varepsilon_{Nd}(t)$=0.42~2.05,相应的两阶段Nd模式年龄(t_{DM2})变化于0.86~0.99 Ga。在$I_{Sr}-\varepsilon_{Nd}(t)$图中样品主要落在亏损地幔(DM)与富集地幔(EM Ⅱ)之间且靠近EM Ⅱ区域,与EM Ⅱ 地幔具有亲源性(图6)。

5 讨　论

5.1 玄武岩岩石成因

分离结晶作用在玄武岩岩浆的演化过程中具有非常重要的作用。马山玄武岩的SiO_2与TiO_2、Fe_2O_3、FeO、MgO、CaO和P_2O_5呈良好的负相关关系,SiO_2与Al_2O_3呈正相关关系;MgO与TiO_2、FeOT、CaO及P_2O_5呈良好的正相关关系,MgO与Al_2O_3、(Na_2O+K_2O)呈良好的负相关关系。同时岩石样品具有低的MgO(3.29%~7.58%)、Ni(5.79×10^{-6}~67.89×10^{-6})、Cr(7.47×10^{-6}~295×10^{-6})、Sc(19.80×10^{-6}~41.18×10^{-6})含量,表明样品中橄榄石、辉石的

表1 马山玄武岩LA-ICPMS锆石U-Pb同位素分析数据

Table 1 LA-ICPMS zircon U-Pb isotopic data of the Mashan basalt

点号	$Pb/10^{-6}$	$Th/10^{-6}$	$U/10^{-6}$	比值(经普通铅校正过的)						年龄(经普通铅校正过的)/Ma					
				$^{207}Pb/^{206}Pb$	$\pm1\sigma$	$^{207}Pb/^{235}U$	$\pm1\sigma$	$^{206}Pb/^{238}U$	$\pm1\sigma$	$^{207}Pb/^{206}Pb$	$\pm1\sigma$	$^{207}Pb/^{235}U$	$\pm1\sigma$	$^{206}Pb/^{238}U$	$\pm1\sigma$
1	52.28	269	1158	0.05505	0.00270	0.29455	0.01366	0.03906	0.00044	414	103	262	11	247	3
2	58.80	286	1195	0.07203	0.00539	0.43508	0.03372	0.04249	0.00085	987	157	367	24	271	5
3	106.50	195	1207	0.07316	0.00155	0.76268	0.01968	0.07465	0.00092	1018	47	576	11	464	6
4	76.30	838	1542	0.05134	0.00129	0.27752	0.00656	0.03918	0.00035	256	51	249	5	248	2
5	16.00	602	508	0.07487	0.00509	0.22180	0.01660	0.02084	0.00028	1065	153	203	14	133	2
6	37.92	227	809	0.05064	0.00182	0.27261	0.00956	0.03905	0.00038	224	80	245	8	247	2
7	55.77	320	1197	0.04923	0.00120	0.26632	0.00628	0.03908	0.00030	159	53	240	5	247	2
8	32.82	236	701	0.04746	0.00124	0.25741	0.00709	0.03912	0.00036	72	60	233	6	247	2
9	36.80	191	818	0.04087	0.00125	0.21971	0.00644	0.03895	0.00032	-240	67	202	5	246	2
10	64.60	327	1029	0.09785	0.06547	0.61612	0.40791	0.04567	0.00441	1584	1424	487	256	288	27
11	269.10	309	1157	0.05564	0.00441	0.31860	0.02509	0.04153	0.00036	438	182	281	19	262	2
12	57.70	304	1254	0.07506	0.00139	2.00108	0.05182	0.19211	0.00360	1070	37	1116	18	1133	19
13	150.10	285	1097	0.06398	0.00663	0.37667	0.03855	0.04270	0.00070	741	229	325	28	270	4
14	308.20	534	3348	0.05283	0.00113	0.28663	0.00629	0.03871	0.00039	322	45	256	5	245	2
15	54.84	335	699	0.10139	0.00174	4.85734	0.08746	0.34062	0.00458	1650	23	1795	15	1890	22
16	62.90	278	1180	0.05164	0.00148	0.28590	0.00933	0.03902	0.00073	269	63	255	7	247	5
17	55.82	384	1317	0.04119	0.00125	0.22694	0.00698	0.03899	0.00080	-222	54	208	6	247	5
18	52.28	300	1166	0.04043	0.00137	0.22465	0.00822	0.03914	0.00099	-265	62	206	7	248	6

分离结晶作用显著;在原始地幔标准化微量元素蛛网图上均表现有弱的Ti和P亏损,表明有钛铁矿和磷灰石分离结晶;SiO_2与Al_2O_3呈正相关关系,球粒陨石标准化稀土元素配分图中缺乏明显的Eu异常,表明没有斜长石的结晶分离。

马山玄武岩的地球化学特征以富集大离子亲石元素(K、Ba、Rb、Sr、Th、U 、LREE),亏损 HREE,无明显的Nb、Ta异常为特征,显示可能受到地壳混染作用。但从另一方面,玄武岩 $Mg^{\#}$值较高,为35.11~56.69,接近于洋中脊拉斑玄武岩的$Mg^{\#}$值(60±,Beard and Lofgren, 1991),玄武岩Nb/Ta平均值为16.44,Zr/Hf平均值为36.97,与原始地幔值(Nb/Ta=17.5、Zr/Hf=36.27)相近,高于大陆地壳平均值(Nb/Ta=11、Zr/Hf=33, Taylor and McLennan, 1985;Stolz et al., 1996)。Th/La平均值为0.18,明显低于大陆地壳的平均值(0.28),稍高于下地壳的Th/La比值(0.15),说明玄武质岩浆上升侵位过程中受到地壳大规模混染程度较小;同位素显示有低I_{Sr}和高$\varepsilon_{Nd}(t)$等反映幔源的特征,随着SiO_2含量的增加,I_{Sr}几乎没有变化,也反映幔源岩浆上侵定位过程中没有发生地壳混染。马山玄武岩具有高的Sr含量(平均值为663.05×10^{-6}),杨祝良等(1999)和曹建劲(2006)分别对浙闽沿海出露的早白垩世玄武岩及广东沿海地区及海南岛基性岩研究发现它们也具有较高的Sr含量,也排除了地壳混染作用。因此,可以判断马山玄武岩其源区主要来自地幔,无明显的地壳混染。

马山玄武岩Nb/U平均值为18.44、Ce/Pb平均值为10.24,明显低于MORB(洋中脊玄武岩)和OIB(洋岛玄武岩)的Nb/U和Ce/Pb比值(分别为40和255,Hofmann et al., 1988),这表明马山玄武岩不可能直接由软流圈地幔部分熔融产生,同时玄武岩的地球化学特征以富集大离子亲石元素(K、Ba、Rb、Sr、Th、U、LREE),亏损Nb、Ta和HREE为特征,同位素显示低I_{Sr}和高$\varepsilon_{Nd}(t)$,与EM Ⅱ地幔具有亲源性。一般认为EM Ⅱ型地幔是俯冲带陆源物质进入上地幔再循环的结果,因为大陆沉积物的同位素特征对于EM Ⅱ地幔的形成最为理想(Zinder and Hart,1986)。因此玄武岩的源区可能与早期俯冲作用带入部分地壳物质进入地幔后,释放流体交代的富集岩石圈地幔有关。Rb、Ba在金云母中为相容元素(LaTourette et al., 1995),Rb、Sr、Ba在角闪石中适

表2 马山玄武岩主量元素(%)和稀土及微量元素(10^{-6})分析结果及参数

Table 2 Compositions and parameters of major elements(%), rare earth and trace element(10^{-6}) in the Mashan basalt

样品号	Mszy-7-1	Mszy-7-4	Mszy-7-5	2803	2806	2809	2812	2818
SiO_2	51.56	49.68	47.30	49.61	48.44	47.95	50.96	46.02
TiO_2	1.59	1.55	2.15	1.24	1.63	2.05	1.83	2.03
Al_2O_3	14.82	12.58	13.21	12.53	12.01	14.75	14.88	13.26
Fe_2O_3	4.81	3.74	4.58	2.99	3.99	7.02	7.71	6.11
FeO	6.33	7.06	7.10	7.43	7.54	5.64	3.90	6.31
MnO	0.18	0.17	0.19	0.16	0.23	0.21	0.13	0.20
MgO	4.23	6.87	6.47	7.43	7.58	4.93	3.29	6.29
CaO	7.48	9.14	8.61	9.14	10.61	7.28	6.19	10.37
Na_2O	3.67	2.50	2.94	1.60	2.17	3.12	3.06	2.53
K_2O	2.74	3.21	2.59	4.35	3.04	3.35	4.96	3.12
P_2O_5	0.58	0.51	0.61	0.54	0.53	0.63	0.59	0.64
H_2O^+	1.40	1.94	2.70					
CO_2	0.11	0.83	1.61					
烧失量	1.31	2.18	3.36	2.49	2.30	2.96	2.30	2.93
总量	99.30	99.19	99.11	99.51	100.07	99.89	99.80	99.81
ALK	6.41	5.71	5.53	5.95	5.21	6.47	8.02	5.65
δ	4.80	4.88	7.11	5.36	4.99	8.46	8.08	10.57
K_2O/Na_2O	0.75	1.28	0.88	2.72	1.40	1.07	1.62	1.23
$Mg^\#$	41.43	54.01	50.69	56.69	54.83	42.36	35.11	48.70
La	51.90	40.00	50.90	29.15	40.60	56.70	52.43	52.44
Ce	97.50	74.10	97.50	56.62	77.70	98.58	98.39	99.77
Pr	11.10	9.18	11.60	7.60	9.79	12.97	12.51	12.35
Nd	44.50	37.40	46.80	30.11	37.04	49.08	47.44	46.21
Sm	7.81	7.09	9.03	6.66	7.53	9.87	9.71	9.32
Eu	2.41	2.12	2.63	1.83	2.17	2.66	2.54	2.59
Gd	7.45	6.92	7.92	5.95	6.63	8.20	8.21	8.02
Tb	1.26	1.16	1.33	0.91	0.98	1.24	1.23	1.12
Dy	7.04	6.29	7.36	5.21	5.24	6.94	6.95	5.98
Ho	1.30	1.14	1.25	1.00	1.02	1.33	1.37	1.16
Er	3.95	3.40	3.72	2.69	2.62	3.44	3.56	2.94
Tm	0.57	0.47	0.56	0.39	0.37	0.47	0.49	0.40
Yb	3.79	3.04	3.49	2.48	2.33	2.96	3.11	2.55
Lu	0.60	0.47	0.55	0.38	0.35	0.45	0.47	0.38
$\sum$REE	241.18	192.78	244.64	150.98	194.37	254.89	248.41	245.23
LREE	215.22	169.89	218.46	131.97	174.83	229.86	223.02	222.68
HREE	25.96	22.89	26.18	19.01	19.54	25.03	25.39	22.55
LREE/HREE	8.29	7.42	8.34	6.94	8.95	9.18	8.78	9.87
$(La/Yb)_N$	9.82	9.44	10.46	8.43	12.50	13.74	12.09	14.75
δEu	0.95	0.91	0.93	0.87	0.92	0.88	0.85	0.89
Ba	747.00	766.00	715.00	1009.70	925.60	938.26	934.74	1032.31
Rb	85.60	124.00	83.90	146.39	98.90	89.12	141.29	162.45
Sr	711.00	695.00	766.00	452.85	640.87	666.64	559.78	812.23
Y	37.10	33.50	36.70	25.53	25.50	36.30	36.71	28.81
Zr	620.00	359.00	651.00	161.23	182.29	223.77	257.02	213.71
Nb	50.70	31.90	52.50	20.09	35.87	46.11	43.59	51.72
Th	9.80	7.13	9.11	6.24	7.74	9.15	10.15	8.30
Pb	15.60	9.11	25.10	4.02	5.60	7.32	9.62	8.30
Ga	20.70	17.40	21.70	16.57	17.98	20.84	18.93	19.28
Ni	25.70	65.50	55.00	64.55	67.89	24.22	5.79	44.99
Cr	57.40	295.00	125.00	161.20	171.82	36.07	7.47	60.34
Hf	14.10	8.72	14.50	4.30	4.85	5.87	6.57	5.71
Sc	19.80	33.70	34.20	41.18	39.47	29.78	22.32	37.62
Ta	2.84	1.72	3.01	1.29	2.30	2.96	2.82	3.34
Co	34.80	43.60	50.20	39.44	47.55	39.77	32.60	47.62
U	2.73	1.96	2.45	1.90	2.01	2.09	3.01	1.97
Rb/Sr	0.12	0.18	0.11	0.32	0.15	0.13	0.25	0.20
Rb/Ba	0.11	0.16	0.12	0.14	0.11	0.09	0.15	0.16
Nb/Ta	17.85	18.55	17.44	15.57	15.60	15.58	15.46	15.49
Zr/Hf	43.97	41.17	44.90	37.50	37.59	38.12	39.12	37.43
Th/U	3.59	3.64	3.72	3.28	3.85	4.38	3.37	4.21

注:玄武岩样品2803、2806、2809、2812、2818引自吴根耀和李曰俊(2011),$\delta=(K_2O+Na_2O)^2/(SiO_2-43)$,$Mg^\#=100\times MgO/(MgO+TFeO)$(摩尔比),$TFeO=FeO+0.8998\times Fe_2O_3$。

表3 马山玄武岩Sr−Nd同位素组成分析结果

Table 3 Sr−Nd isotopic data of the Mashan basalt

样号	Sm/10^{-6}	Nd/10^{-6}	^{147}Sm/^{144}Nd	^{143}Nd/^{144}Nd	2σ	$\varepsilon_{Nd}(t)$	t/Ma
Mszy-7-1	8.318	45.57	0.111095	0.512589	0.000005	1.74	246.7
Mszy-7-4	7.336	37.30	0.119703	0.512535	0.000004	0.42	246.7
Mszy-7-5	8.224	44.04	0.113655	0.512609	0.000006	2.05	246.7
样号	Rb/10^{-6}	Sr/10^{-6}	^{87}Rb/^{86}Sr	^{87}Sr/^{86}Sr	2σ	(^{87}Sr/^{86}Sr)$_i$	t_{DM2}(Ga)
Mszy-7-1	91.45	757.80	0.34033	0.70603	0.00004	0.704834	0.88
Mszy-7-4	134.50	726.30	0.52224	0.70651	0.00004	0.704675	0.99
Mszy-7-5	84.39	786.50	0.30259	0.70566	0.00002	0.704597	0.86

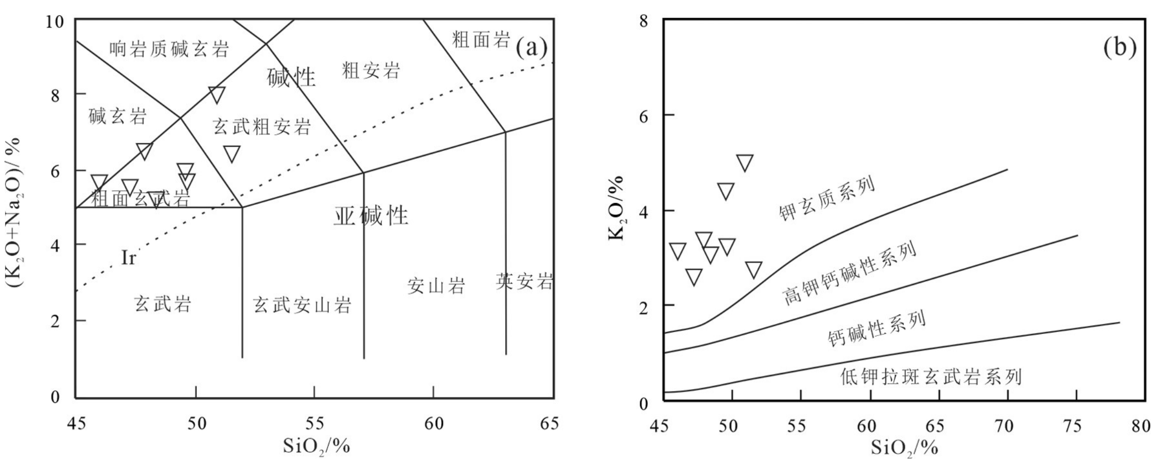

图4 马山玄武岩分类判别图解（a据Le Bas et al., 1986；b据Peccerillo and Taylor, 1976）

Fig.4 Classifications diagrams of the Mashan basalt (a after Le Bas et al., 1986; b after Peccerillo and Taylor, 1976)

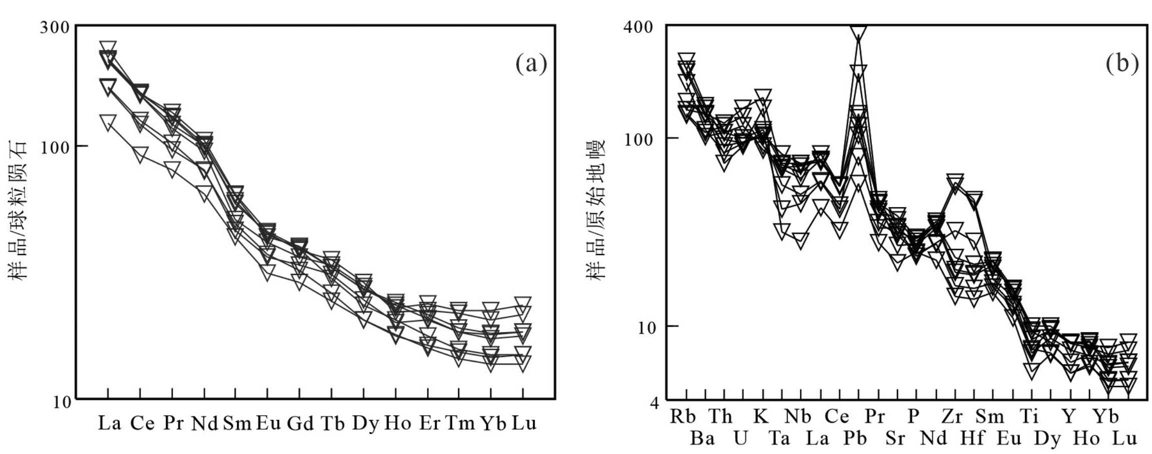

图5 马山玄武岩稀土元素球粒陨石标准化配分图及微量元素原始地幔标准化蛛网图（标准化数值据Sun and Mcdonough, 1989）

Fig.5 Chondrite−normalized REE patterns and primitive mantle−normalized trace elements spider diagrams of the Mashan basalt (normalized values are from Sun and McDonough, 1989)

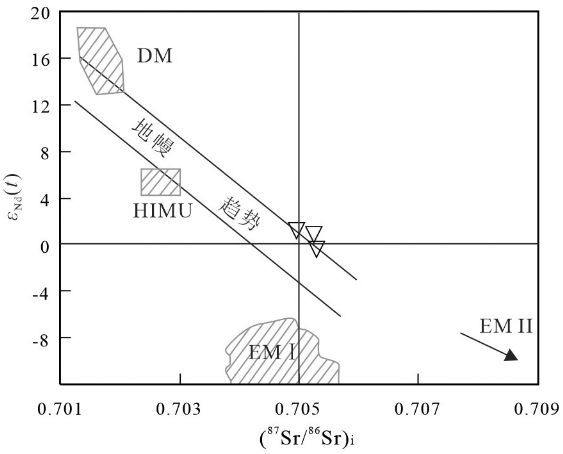

图6 马山玄武岩I_{Sr}−$\varepsilon_{Nd}(t)$关系图(底图据Zinder and Hart, 1986)

DM—亏损地幔;HIUM—高U/Pb比值地幔;EM Ⅰ—Ⅰ型富集地幔;EM Ⅱ—Ⅱ型富集地幔

Fig.6 I_{Sr}−$\varepsilon_{Nd}(t)$ diagram of the Mashan basalt (after Zinder and Hart, 1986)

DM−Depleted mantle; HIUM−High U/Pb ratio mantle; EM Ⅰ−Enriched mantle I; EM Ⅱ−Enriched mantle II

度相容(Adam et al., 1993;LaTourette et al., 1995),Nb在角闪石中比在金云母中更相容(LaTourette et al., 1995; Ionov et al., 1997)。所以可以根据金云母和角闪石中微量元素的差异性,来判断岩浆熔融的岩石圈源区是角闪石还是金云母(Furman and Graham, 1999; Yang et al., 2005; Xia and Xu, 2005)。Ba/Rb−Rb/Sr和Nb/Th−Rb/Sr图解显示,马山玄武岩样品几乎都落在金云母的趋势范围(图7),说明玄武岩的源区主要的含水矿物相为金云母。微量元素HREE、Y在石榴石中强烈富集,而角闪石相对富集中稀土元素(MREE)(Green, 1994),尖晶石则强烈亏损REE及Y(Glaser et al., 1999)。因此,马山玄武岩亏损HREE,表明其源区残留相主要是石榴石,判断马山玄武岩的岩浆来源于石榴石相地幔的部分熔融。在地幔中尖晶石相转变为石榴石相的转换深度约为60~80 km,石榴石相的稳定上限为70~80 km、角闪石相稳定下限约为80 km(Wendlant and Eggler, 1980; Olafsson and Eggler, 1983),因此马山玄武岩的源区成分为含金云母石榴石橄榄岩,源区深度应大于80 km,对含金云母的矿物集合体稳定性评估实验证明,熔体形成于近3000~3500 MPa,或者说深度90~100 km(Olafsson and Eggler, 1983; Wallace and Green, 1988; Lloyd et al., 1991; Sato et al., 1997)。因此玄武质岩浆可能起源于约80~100 km。

5.2 构造意义

马山玄武岩样品在Zr−Zr/Y玄武岩判断图解上主要落在板内玄武岩区(图8a),在玄武岩类Ta/Hf−Th/Hf大地构造环境判别图落在陆内裂谷碱性玄武岩区(图8b),因此可以判断马山玄武岩产于板内环境。

扬子和华夏地块在新元古代(约820 Ma)拼合之后直到晚古生代—早中生代华南地区再无新的洋壳打开,华南自约820 Ma后进入板内或陆内演化阶段(舒良树, 2006; Wang et al., 2010; Li et al.,

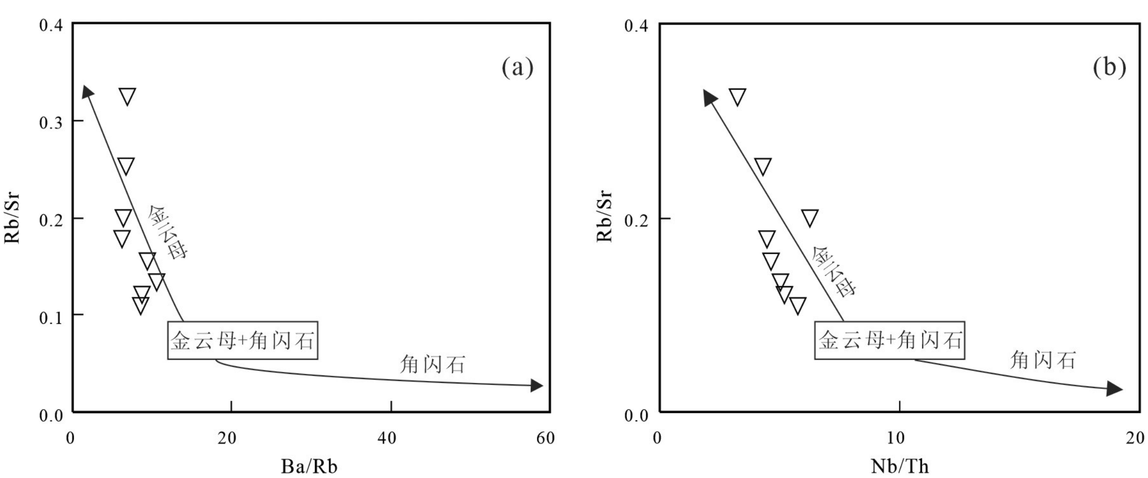

图7 马山玄武岩Ba/Rb−Rb/Sr和Nb/Th−Rb/Sr图解(底图据Furman and Graham, 1999)

Fig.7 Ba/Rb−Rb/Sr and Nb/Th−Rb/Sr diagrams of the Mashan basalt (after Furman and Graham, 1999)

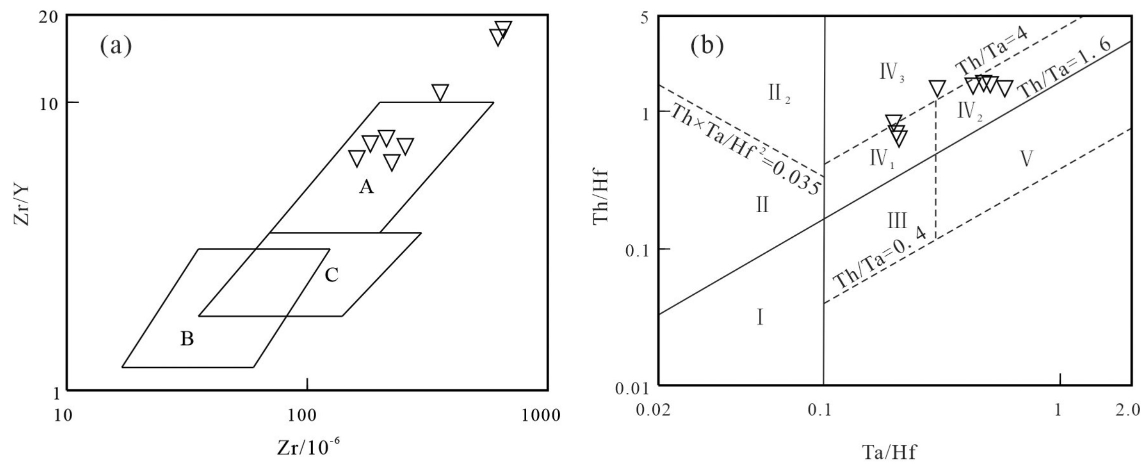

图8 马山玄武岩构造环境判别图解(底图a据Pearce and Norry, 1979;底图b据汪云亮等,2001)

A—板内玄武岩区;B—岛弧玄武岩区;C—洋中脊玄武岩区;Ⅰ—板块发散边缘N-MORB区;Ⅱ—板块汇聚边缘(Ⅱ$_1$—大洋岛弧玄武岩区;Ⅱ$_2$—陆缘岛弧及陆缘火山弧玄武岩区);Ⅲ—大洋板内洋岛、海山玄武岩区及T-MORB、E-MORB区;Ⅳ—大陆板内(Ⅳ$_1$—陆内裂谷及陆缘裂谷拉斑玄武岩区;Ⅳ$_2$—陆内裂谷碱性玄武岩区;Ⅳ$_3$—大陆拉张带(或初始裂谷)玄武岩区);Ⅴ—地幔热柱玄武岩区

Fig.8 Tectonic setting discrimination diagrams of the Mashan basalt (a after Pearce and Norry, 1979; b after Wang Yunliang et al., 2001)

A-Within-plate basalt; B-Island arc basalt; C-Mid-ocean ridge basalt; Ⅰ-N-MORB; Ⅱ-Plate convergence margin (Ⅱ$_1$-Oceanic island basalt; Ⅱ$_2$-Volcanic arc basalt); Ⅲ-Oceanic intraplate island basalt, seamount basalt and T-MORB, E-MORB; Ⅳ-Intraplate basalt (Ⅳ$_1$-Intracontinental rift basalt and continental margin rift tholeiite; Ⅳ$_2$-Alkali basalt; Ⅳ$_3$-Incipient rift basalt); Ⅴ-Mantle plume basalt

2010),印支期造山为板内或陆内造山,但其造山机制或驱动力还有待进一步研究。印支期发育的含石榴石堇青石强过铝S型花岗岩只出露于桂东南十万大山—大容山一带,而华南其他地区出露的印支期花岗岩只是一些过铝质花岗岩(周岱等,2021)。S型过铝质花岗岩被认为不仅与碰撞挤压环境下的地壳加厚有关,也是后碰撞伸展环境的标志。Guo et al.(1997)认为湖南印支期花岗岩的形成可能与区内印支期幔源玄武质岩浆对中下地壳的烘烤所导致的地壳重熔有关,并非碰撞挤压所形成。Wang et al.(2002)认为湖南印支期过铝质花岗岩的形成与玄武质岩浆的底侵有关。Wang et al.(2003)认为武夷山洋坊242 Ma的霓辉石正长岩形成于印支期伸展环境。Sibumasu地块向印支-华南地块斜向汇聚的主碰撞期为243~258 Ma(Carter et al., 2001),马山玄武岩的LA-ICPMS锆石的U-Pb年龄为(246.7±1.5)Ma,其时代与印支运动结束的时代基本一致,地球化学特征显示其为钾玄质岩石,构造环境判断其产于板内裂谷环境,同时又远离Song ma碰撞缝合带及古太平洋板块向华南大陆之下俯冲带,所以其形成机制和印支板块碰撞及太平洋板块的俯冲作用可能关系不大。桂东南地区灵山断裂、岑溪—博白断裂、罗定—广宁断裂、信宜—廉江断裂、吴川—四会断裂等印支期的逆冲-推覆构造十分发育,云开大山周边断裂带的同位素测年为200~256 Ma(彭少梅等,1995;Wang et al., 2007)。因此,马山玄武岩更可能与桂东南地区逆冲-推覆构造后期的伸展作用有关,由于伸展作用产生有利空间,造成玄武质岩浆上侵并喷发,形成马山玄武岩。

6 结 论

(1)马山玄武岩形成年龄为(246.7±1.5)Ma,为早三叠世印支期玄武岩。

(2)马山玄武岩富碱、富钾,为钾质粗面玄武岩。稀土元素特征为轻稀土富集型,微量元素特征为富集大离子亲石元素,亏损高场强元素,为钾玄岩系列岩石。其岩浆作用以分离结晶为主,无明显的地壳混染。Sr-Nd同位素显示具有EM Ⅱ富集地幔端元的特征,其源区为早期俯冲作用带入的部分地壳物质进入地幔后,经流体交代作用形成含金云母石榴石的富集地幔(>80 km)源区。

(3)马山玄武岩产于板内环境,其形成可能与桂东南地区印支期逆冲-推覆构造后期的伸展作用有关,由于伸展作用产生有利空间,造成玄武岩浆

上侵并喷发并形成玄武岩。

注释

❶广西壮族自治区区域地质调查研究院. 2006. 广西1:25万玉林市幅区域地质调查报告[R]. 1−687.

References

Adam J D, Green T H, Sie S H. 1993. Proton microprobe determined partitioning of Rb, Sr, Ba, Y, Zr, Nb and Ta between experimentally produced amphiboles and silicate melts with variable F content[J]. Chemical Geology, 109(1/4): 29−49.

Beard J S, Lofgren G E. 1991. Dehydration melting and water−saturated melting of basaltic and andesitic greenstones and amphibolites at 1, 3, and 6.9 kb[J]. Journal of Petrology, 32(2): 365−401.

Campbell I H. 2007. Testing the plume theory[J]. Chemical Geology, 241(3/4): 153−176.

Carter A, Roques D, Bristow C, Kinny P. 2001. Understanding Mesozoic accretion southeast Asia: Significance of Triassic thermotectonism (Indosinian orogeny) in Vietnam[J]. Geology, 29 (3): 211−214.

Cao Jianjin. 2006. Geochemistry of the Mesozoic and Cenozoic Mafic Dikes and the Lithosphere Revolution from the Coastal Areas of Guangdong Province and Hainan Island, China[D]. Guiyang: Institute of Geochemistry, Chinese Academy of Sciences, 1−126 (in Chinese with English abstract).

Chen Lihui, Zeng Gang, HU Senlin, Yu Xun, Chen Xiayu. 2012. Crustal recycling and genesis of continental alkaline basalts: Case study of the Cenozoic alkaline basalts from Shandong Province, eastern China[J]. Geological Journal of China Universities, 18(1): 16−27 (in Chinese with English abstract).

Furman T, Graham D. 1999. Erosion of lithospheric mantle beneath the East African Rift system: Geochemical evidence from the Kivu volcanic province[J]. Lithos, 48(1/4): 237−262.

Glaser S M, Foley S F, Günther D. 1999. Trace element compositions of minerals in garnet and spinel peridotite xenoliths from the Vitim volcanic field, Transbaikalia, eastern Siberia[J]. Lithos, 48(1/4): 263−285.

Green T H. 1994. Experimental studies of trace−element partitioning applicable to igneous petrogenesis Sedona 16 years later[J]. Chemical Geology, 117(1/4): 1−36.

Guo F, Fan W M, Lin G, Lin Y X. 1997. Sm−Nd dating and petrogenesis of Mesozoic gabbro xenolith in Daoxian County, Hunan Province[J]. Chinese Science Bulletin, 42(21): 1814−1816.

Guo Xinshen, Chen Jiangfeng, Zhang Xun, Tang Jiafu, Xie Zhi, Zhou Taixi, Liu Yulong. 2001. Nd isotopic ratios of K−enriched magmatic complexes from southeastern Guangxi Province: Implications for upwelling of the mantle in southeastern China during the Mesozoic[J]. Acta Petrological Sinica, 17(1): 19−27 (in Chinese with English abstract).

Hofmann A W. 1988. Chemical differentiation of the Earth: The relationship between mantle, continental crust, and oceanic crust[J]. Earth and Planetary Science Letters, 90(3): 297−314.

Ionov D A, Griffin W L, O'Reilly S Y. 1997. Volatile−bearing minerals and lithophile trace elements in the upper mantle[J]. Chemical Geology, 141(1/4): 153−184.

LaTourette T, Hervig R L, Holloway J R. 1995. Trace element partitioning between amphibole, phlogopite, and basanite melt[J]. Earth and Planetary Science Letters, 135(5/6): 13−30.

Le Bas M J, Le Maitre R W, Streckeisen A, Zanettin B. 1986. A chemical classification of volcanic rocks based on the total Alkali−Silica diagram[J]. Journal of Petrology, 27(3): 745−750.

Li X H, Zhou H W, Liu Y, Lee C, Sun M, Chen C H. 2000. Shoshonitic intrusive suite in SE Guangxi: Petrology and geochemistry[J]. Chinese Science Bulletin, 45(7): 653−659.

Li Z X, Li X H, Wartho J A, Clark C, Li W X, Zhang C L, Bao C D. 2010. Magmatic and metamorphic events during the early Paleozoic Wuyi−Yunkai orogeny, southeastern South China: New age constraints and pressure−temperature conditions[J]. GSA Bulletin, 122(1/4): 772−793.

Li Zilong, Yang Shufeng, Chen Hanlin, Yu Xin, Langmuir C H. 2008. Chronology and geochemistry of Taxinan basalts from the Tarim basin: Evidence for Permian plume magmatism[J]. Acta Petrologica Sinica, 24(S1): 959−970 (in Chinese with English abstract).

Liu Yong, Li Tingdong, Xiao Qinghui, Geng Shufang, Wang Tao, Chen Bihe. 2010. New chronology of the Ningyuan alkali basalt in southern Hunan, China: Evidence from LA−ICP−MS zircon U−Pb dating[J]. Geological Bulletin of China, 29(6): 833−941 (in Chinese with English abstract).

Lloyd F E, Huntingdon A T, Davies G R, Nixon P H. 1991. Phanerozoic volcanism of Southwest Uganda: A Case for Regional K and LILE Enrichment of the Lithosphere beneath a Domed and Rifted Continental Plate. In: Kampunzu A B, Lubala R T(eds.). Magmatism in Extensional Structural Settings: The Phanerozoic African Plate[M]. Berlin Springer, 23−72.

Lu Yuanfa, Li Wenxia. 2021. Petrochemical calculation method and VBA program for natural mineral of granitoids[J]. South China Geology, 37(4): 445−457 (in Chinese with English abstract).

Nielsen T F D, Turkov V A, Solovova I P, Kogarko L N, Ryabchikov I D. 2006. A Hawaiian beginning for the Iceland plume: Modelling of reconnaissance data for olivine−hosted melt inclusions in Palaeogene picrite lavas from East Greenland[J]. Lithos, 92(1): 83−104.

Olafsson M, Eggler D H. 1983. Phase relations of amphibole, amphibole−carbonate and phlogopite−carbonate peridotite: Petrologic constraints on the asthenosphere[J]. Earth and Planetary

Science Letters, 64 (2): 305−315.

Pearce J A, Norry M J. 1979. Petrogenetic implications of Ti, Zr, Y and Nb variations in volcanic rocks[J]. Contributions to Mineralogy and Petrology, 69(1): 33−47.

Peccerillo A, Taylor S R. 1976. Geochemistry of Eocene calc−alkaline volcanic rocks from the Kastamonu area, northern Turkey[J]. Contributions to Mineralogy and Petrology, 58(1): 63−81.

Peng Shaomei, Peng Songbai, Shao Jianguo. 1995. Geological features and tectonic evolution of peripheral faults around Yunkai Massif[J]. Guangdong Geology, 10(2): 9−16 (in Chinese with English abstract).

Sato K, Katsura T, Ito E. 1997. Phase relations of natural phlogopite with and without enstatite up to 8 GPa: Implications for mantle metasomatism[J]. Earth and Planetary Science Letters, 146(3/4): 511−526.

Shu Liangshu. 2006. Pre−Devonian tectonic evolution of South China: From Cathaysian Block to Caledonian period folded orogenic belt[J]. Geological Journal of China Universities, 12(4): 418−431 (in Chinese with English abstract).

Stolz A J, Jochum K P, Spettel B, Hofmann A W. 1996. Fluid− and melt−related enrichment in the subarc mantle: Evidence from Nb/Ta variations in island−arc basalts[J]. Geology, 24(7): 587−590.

Sun S S, McDonough W F. 1989. Chemical and isotopic systematics of oceanic basalts: Implications for mantle compositions and processes[J]. Geological Society London Special Publications, 42 (1): 313−345.

Taylor S R, McLennan S M. 1985. The Continental Crust: Its Composition and Evolution[M]. Boston: Blackwell Scientific Publication, 209−230.

Wallace M E, Green D H. 1988. An experimental determination of primary carbonatite composition[J]. Nature, 335(6188): 343−345.

Wang Q, Zhao Z H, Jian P, Xiong X L, Ma Ji L, Bao Z W. 2003. SHRIMP U−Pb zircon geochronology of Yangfang aegiriteaugite syenite in Wuyi Mountains of South China and its tectonic implications[J]. Chinese Science Bulletin, 48(20) :2241−2247.

Wang Xiaodi. 2013. A study on geochronology, geochemistry and genesis of Mashan Complex, Southeast Guangxi [D]. Chengdu: Chengdu University of Technology, 1− 129 (in Chinese with English abstract).

Wang Yinxi, Yang Jiedon, Tao Xiangchong, Li Huimin. 1988. A study of the Sm− Nd method for fossil mineral and rock and its applications[J]. Journal of Nanjing University (Natural Science), 24 (2): 297−308 (in Chinese with English abstract).

Wang Y J, Zhang Y H, Fan W M, Xi X W, Guo F, Lin G. 2002. Numerical modeling of the formation of Indo−Sinian peraluminous granitoids in Hunan Province: Basaltic underplating versus tectonic thickening[J]. Science in China (Series D: Earth Sciences), 45(11): 1042−1056.

Wang Y J, Fan W M, Cawood P A, Ji S C, Peng T P, Chen X Y. 2007. Indosinian high−strain deformation for the Yunkaidashan tectonic belt, south China: Kinematics and $^{40}Ar/^{39}Ar$ geochronological constraints[J]. Tectonics, 26(6): 229−247.

Wang Y J, Zhang F F, Fan W M, Zhang G W, Chen X Y, Cawood P A, Zhang A M. 2010. Tectonic setting of the South China Block in the early Paleozoic: Resolving intracontinental and ocean closure models from detrital zircon U−Pb geochronology[J]. Tectonics, 29 (10): 1−16.

Wang Yuejun, Liao Chaolin, Fan Weiming, Peng Touping. 2004. Early Mesozoic OIB−type alkaline basalt in central Jiangxi Province and its tectonic implications[J]. Geochimica, 33(2): 109− 117 (in Chinese with English abstract).

Wang Yunliang, Zhang Chengjiang, Xiu Shuzhi. 2001. Th/Hf− Ta/Hf identification of tectonic setting of basalts[J]. Acta Petrologica Sinica, 17(3): 413−421 (in Chinese with English abstract).

Wendlant R F, Eggler D H. 1980. The origins of potassic magmas: Stability of phlogopite in natural spinel lherzolite and in the system $KAlSiO_4$− MgO− SiO_2− H_2O− CO_2 at high pressures and high temperatures[J]. American Journal of Science, 280(5): 421−458.

Wu Genyao, Li Yuejun. 2011. The Mashan Indosinian oceanic island basalt outcropping along the Lingshan fracture in Southeast Guangxi and its tectonic implications[J]. Geoscience, 25(4): 682−691 (in Chinese with English abstract).

Xia P, Xu Y G. 2005. Domains and enrichment mechanism of the lithospheric mantle in western Yunnan: A comparative study on two types of Cenozoic ultrapotassic rocks[J]. Science in China, 48(3): 326−337.

Xu Yigang. 2006. Using basalt geochemistry to constrain Mesozoic−Cenozoic evolution of the lithosphere beneath North China Craton[J]. Earth Science Frontiers, 13(2): 93−104 (in Chinese with English abstract).

Yang J H, Chung S L, Wilde S A, Wu F W, Chu M F, Lo C H, Fan H R. 2005. Petrogenesis of post− orogenic syenites in the Sulu Orogenic Belt, East China: Geochronological, geochemical and Nd−Sr isotopic evidence[J]. Chemical Geology, 214(1/2): 99−125.

Yang Zhuliang, Shen Weizhou, Tao Kuiyuan, Shen Jiaolin. 1999. Sr, Nd and Pb isotopic characteristics of Lower Cretaceous basalts from the coast of Zhejiang and Fujian, China: Evidence for ancient enriched mantle source[J]. Scientia Geologica Sinica, 34(1): 59−68 (in Chinese with English abstract).

Yu Xinqi, Shu Liangshu, Deng Guohui, Wang Bin, Zhu Fuping. 2005. Geochemical features and tectonic significance of the alkali−basalts from Ji'an−Taihe basin, Jiangxi Province[J]. Geoscience, 19 (1): 133−140 (in Chinese with English abstract).

Yuan H L, Wu F Y, Gao S, Liu X M, Xu P, Sun D Y. 2003. Determination of U−Pb age and rare earth element concentrations of zircons from Cenozoic intrusions in northeastern China by laser ablation ICP−MS[J]. Chinese Science Bulletin, 48(22): 2411−2421.

Zhao Hui, Yang Jingsui, Liu Fei, Xiong Fahui, Zhang Lan, Lian Dongyang. 2015. Geochemical and chronological studies of the alkaline basalt in Saga along the Yarlung Zangbo suture zone, Tibet[J]. Geology in China, 42(5): 1242−1256 (in Chinese with English abstract).

Zhao Zhenhua, Bo Zhiwei, Zhang Boyou. 1998. Geochemistry of the Mesozoic basaltic rocks in southern Hunan Province[J]. Scientia Sinica(Terrae), 28(S2): 7−14 (in Chinese).

Zhou Dai, Hu Jun, Yang Wenqiang, Chen Qi, Wang Xiangdong, Wang Lei, Xu Deming. 2021. Formation age and petrogenesis of the Xinxing pluton in western Guangdong: Constraint on the closure of the East Paleo−Tethys Ocean[J]. Geology in China, 48(6): 1896−1923 (in Chinese with English abstract).

Zinder A, Hart S R. 1986. Chemical geodynamics[J]. Annual Review of Earth and Planetary Sciences, 14(1): 493−571.

附中文参考文献

曹建劲. 2006. 广东沿海地区及海南岛中新生代基性岩脉地球化学与岩石圈演化[D]. 贵阳: 中国科学院地球化学研究所, 1−126.

陈立辉, 曾罡, 胡森林, 俞恂, 陈霞玉. 2012. 地壳再循环与大陆碱性玄武岩的成因: 以山东新生代碱性玄武岩为例[J]. 高校地质学报, 18(1): 16−27.

郭新生, 陈江峰, 张巽, 汤加富, 谢智, 周泰禧, 刘玉龙. 2001. 桂东南富钾岩浆杂岩的Nd同位素组成: 华南中生代地幔物质上涌事件[J]. 岩石学报, 17(1): 19−27.

厉子龙, 杨树锋, 陈汉林, 余星, Langmuir C H. 2008. 塔西南玄武岩年代学和地球化学特征及其对二叠纪地幔柱岩浆演化的制约[J]. 矿物岩石地球化学通报, 27(S1): 959−970.

刘勇, 李廷栋, 肖庆辉, 耿树方, 王涛, 陈必河. 2010. 湘南宁远地区碱性玄武岩形成时代的新证据: 锆石LA−ICP−MS U−Pb定年[J]. 地质通报, 29(6): 833−941.

路远发, 李文霞. 2021. 花岗岩类自然矿物岩石化学换算及程序设计[J]. 华南地质, 37(4): 445−457.

彭少梅, 彭松柏, 邵建国. 1995. 云开地块周边断裂带的地质特征与构造演化[J]. 广东地质, 10(2): 9−16.

舒良树. 2006. 华南前泥盆纪构造演化: 从华夏地块到加里东期造山带[J]. 高校地质学报, 12(4): 418−431.

王晓地. 2013. 桂东南马山杂岩的年代学、地球化学及成因研究[D]. 成都: 成都理工大学, 1−129.

王银喜, 杨杰东, 陶仙聪, 李惠民. 1988. 化石、矿物和岩石样品的Sm−Nd同位素实验方法研究及其应用[J]. 南京大学学报(自然科学版), 24(2): 297−308.

王岳军, 廖超林, 范蔚茗, 彭头平. 2004. 赣中地区早中生代OIB碱性玄武岩的厘定及构造意义[J]. 地球化学, 33(2): 109−117.

汪云亮, 张成江, 修淑芝. 2001. 玄武岩类形成的大地构造环境的Th/Hf−Ta/Hf图解判别[J]. 岩石学报, 17(3): 413−419.

吴根耀, 李曰俊. 2011. 桂东南马山沿灵山断裂出露的印支期洋岛玄武岩及其区域构造意义[J]. 现代地质, 25(4): 682−691.

徐义刚. 2006. 用玄武岩组成反演中—新生代华北岩石圈的演化[J]. 地学前缘, 13(2): 93−104.

杨祝良, 沈渭洲, 陶奎元, 沈加林. 1999. 浙闽沿海早白垩世玄武岩锶、钕、铅同位素特征——古老富集型地幔的证据[J]. 地质科学, 34(1): 59−68.

余心起, 舒良树, 邓国辉, 王彬, 祖辅平. 2005. 江西吉泰盆地碱性玄武岩的地球化学特征及其构造意义[J]. 现代地质, 19(1): 133−140.

赵慧, 杨经绥, 刘飞, 熊发挥, 张岚, 连东洋. 2015. 西藏雅鲁藏布江缝合带萨嘎碱性玄武岩地球化学和年代学研究[J]. 中国地质, 42(5): 1242−1256.

赵振华, 包志伟, 张伯友. 1998. 湘南中生代玄武岩类地球化学特征[J]. 中国科学(D辑:地球科学), 28(S2): 7−14.

周岱, 胡军, 杨文强, 陈奇, 王祥东, 王磊, 徐德明. 2021. 粤西新兴岩体的形成时代与成因研究:对古特提斯洋东支关闭时间的约束[J]. 中国地质, 48(6): 1896−1923.